

Novel x-cut lithium niobate intensity modulator with 10G bandwidth

Yasuyuki Miyama, Tohru Sugamata, Yoshihiro Hashimoto, Toshihiro Sakamoto, and Hirotohi Nagata

Optoelectronics Research Group, New Technology Research Laboratories,
Sumitomo Osaka Cement Co., Ltd.
585 Toyotomi-cho, Funabashi-shi, Chiba 274-8601, Japan

ABSTRACT

To fabricate a low-driving voltage, high-speed x-cut lithium niobate modulator with 50-ohm electrode impedance, we introduce a novel design approach, which employs a patterned SiO₂ buffer layer. Experimental results showed that the partial removal of SiO₂ buffer layer was effective in both lowering driving voltage and suppressing dc-drift of the modulators.

Keywords: x-cut lithium niobate modulator, patterned SiO₂ buffer layer, 10G bandwidth, lower driving voltage, dc-drift suppression

1. INTRODUCTION

Lithium niobate (LN) optical modulators, such as x-cut or z-cut LN Mach-Zehnder intensity modulators, are critical devices for WDM systems. To meet the needs of current WDM system technology, a low-driving voltage, high-speed x-cut LN modulator is required. In order to reduce driving voltage, conventional x-cut LN modulators are designed to have a wide hot (signal) electrode and a narrow gap between the hot and the ground electrodes. With such electrode geometry, velocity matching between the lightwave and microwave is difficult to achieve because the effective refractive index of microwave tends to be higher than that of the lightwave. This velocity mismatch is the cause for the narrow bandwidth typically found in conventional x-cut LN modulators. In addition to narrow bandwidth, the characteristic impedance of this electrode geometry tends to be close to 25 ohm, which produces an unacceptably high microwave reflection in operation with a standard 50-ohm driver. Thus, the conventional x-cut LN modulator with a 25-ohm electrode might not be suitable for high-speed modulation up to 10G b/s. However, high-speed x-cut LN modulators with a 50-ohm electrode also pose a problem in that they require higher driving voltages than that of x-cut LN modulators with a 25-ohm electrode. In order to achieve both velocity and impedance matching in x-cut LN modulators, the width of the hot electrode should be narrower and the electrode gap should be wider. With this electrode geometry, we can expect a decrease in efficiency in the interaction between the lightwave and microwave, which will produce a higher driving voltage in the x-cut LN modulators. Therefore, while low-driving voltage and high-speed modulation can be achieved independently, the difficulty is achieving both in the same modulator design.

In order to overcome the above-mentioned limitations and realize a low-driving voltage, high-speed x-cut LN

modulator with 50-ohm electrode impedance, we propose a novel device design, which employs a patterned SiO₂ buffer layer. We fabricated a device using this design, and partial removal of SiO₂ buffer layer was shown to be effective in both lowering the driving voltage and suppressing dc-drift of the modulators.

2. DESIGN CONCEPT

The concept for a patterned SiO₂ buffer layer configuration was derived from our hypothesis that the performance of coplanar electrodes is more dependent on the distribution of the dielectric constant around the hot electrode and less so around the ground electrodes. Partial removal of SiO₂ buffer layer between the electrodes would be equivalent to replacing the buffer layer with an air layer, which has a lower dielectric constant than that of SiO₂ buffer layer. The partial removal would cause the electric field of microwave to concentrate on more of the LN substrate surface area and be effective in improving the interaction between lightwave and microwave. This effect is schematically shown in Figure 1.

However, in our preliminary experiments, we found that when the exposed electrode gaps of the SiO₂ buffer layer were dry-etched, using the electrodes themselves as a mask, the driving voltage of the etched sample was increased in comparison to our measurements before etching. This result might be caused by the complete replacement of the buffer layer exposed between electrode gaps with an air layer, which might produce too high a concentration of electric field of microwave into the strict area around the hot electrode, and results in a decrease in the efficiency of the interaction between lightwave and microwave. Due to these preliminary results, we consider that there would be an optimum width for the remaining buffer layer to achieve a lower driving voltage of the modulator.

Another predicted advantage of this configuration was that partial removal of the SiO₂ buffer layer would be effective in suppressing dc-drift in the modulator. Yamada and Minakata showed that the short time dc-drift of an optical device was suppressed by buffer layer separation between the electrodes¹. Although the precise mechanism of dc-drift phenomenon is still uncertain, it is generally understood that the electric carrier generated in dielectric material, such as a LN substrate and a buffer layer, is the main cause of this phenomenon. Especially, the buffer layer has a strong influence on total drive voltage of the modulator². Therefore, we can expect that buffer layer removal will produce a positive effect in suppressing dc-drift.

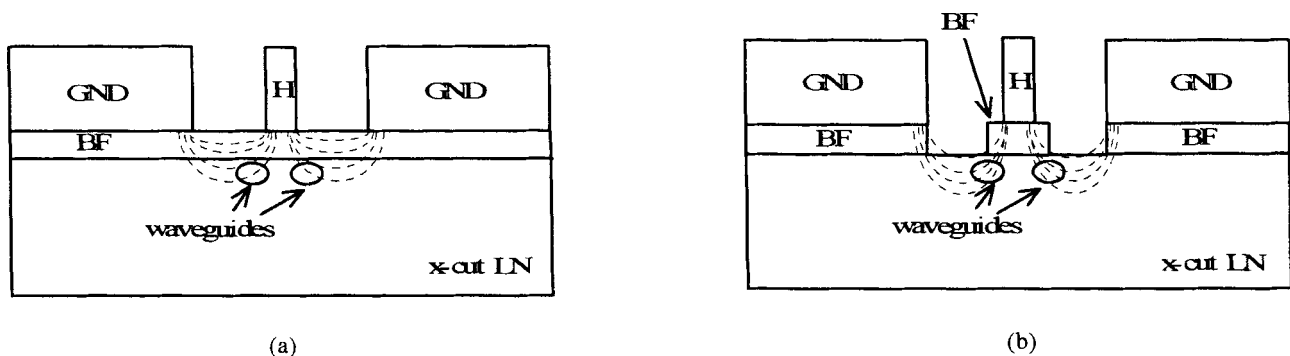


Figure 1 Schematic cross-sections of x-cut LN intensity modulator showing the effect of removing buffer layer exposed between the electrodes. (a) having a conventional planar buffer layer and (b) having a partially removed buffer layer.

3. EXPERIMENTAL RESULTS AND DISCUSSIONS

3.1 Damage Evaluation of Waveguide by Plasma Etching

For patterning the buffer layer we employed plasma dry etching technique with fluorocarbon gas because this was superior to chemical etching technique in precise productivity and reproducibility. In addition, a dry process might be freer from impurity contamination to the buffer layer than a wet one. However, there was a worry about damage of waveguides because they would be exposed to plasma attack when the buffer layer lvas over-etched. Thus, at first, waveguide damage by excess plasma attack was evaluated.

Ti-indiffused straight waveguides fabricated on x-cut LN substrate Tvere prepared. After optical end-suface was formed, insertion loss and a mode profile of the waveguides were measured at wavelength = 1.55 μ m. Then. this waveguide sample was partially masked by polyimide film, exposing length being 50mm. The waveguide sample was repeatedly exposed to plasma at intervals of 300 seconds and their insertion loss and mode profiles were measured after each etching batch, The total time of plasma etching was up to 1800 seconds, and it was equal to 440nm etching depth of LN substrate.

Figures 2(a) and 2(b) show the experimental results of etching time versus insertion loss and mode profile, respectively. Though insertion loss of waveguide gradually increased in accordance with increase of etching time, it seemed to be not serious because averaged excess loss of the samples was 0.14dB at 600 seconds and 0.39dB at 1200 seconds. The mode profile of waveguide scarcely changed except for a slight extension of vertical field. From these results, we considered that the damage of waveguide by plasma attack could be negligible under practical sample treatment.

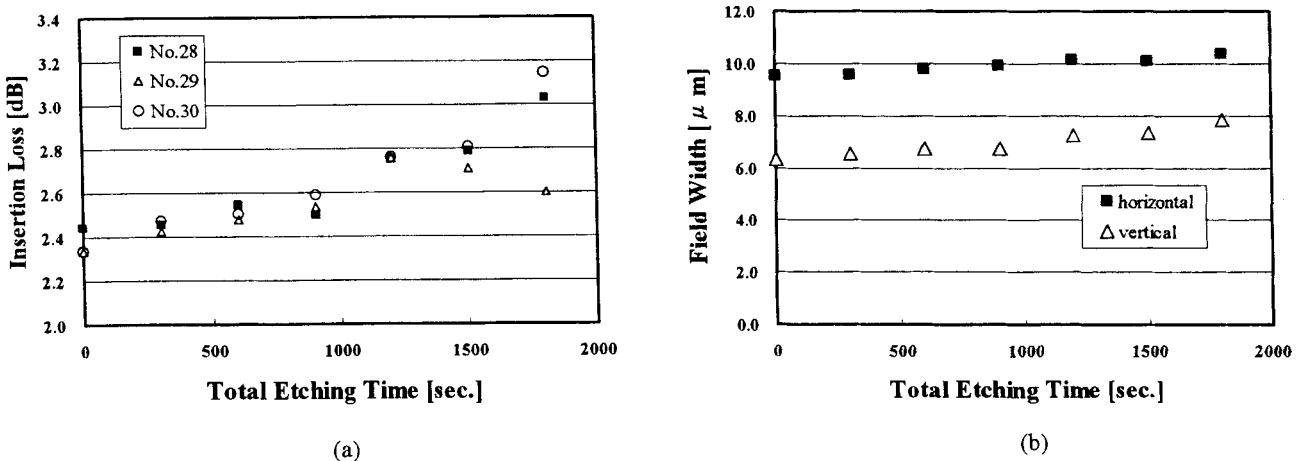


Figure 2 Experimental results of damage evaluation of 11 waveguide by plasma etching
(a) for insertion loss of three waveguides and (b) for mode profile.

3.2 Optimizing Etching Pattern of Buffer Layer

For the experiment of optimizing etching pattern of buffer layer x-cut v-propagating Mach-Zehnder waveguides were fabricated using Ti indiffusion technique. Ti stripes which had about 90nm-thickness and 7 μm -width were indiffused at 1000°C for 15 hours. A SiO₂ buffer layer (with about 1 μm -thick) was fabricated on the waveguide by vacuum evaporation and subsequently annealed at 600°C for 5 hours. As already mentioned in the previous section, plasma dry etching technique was used for buffer layer patterning. During the dry etching process, Cr film for a dry etching mask was firstly deposited on the buffer layer and patterned using the photolithography and chemical etching techniques. After fabrication of Cr-film mask, the buffer layers were patterned by an electron cyclotron resonance (ECR) plasma etching apparatus. CF₄ was used for a parent gas of the plasma. After dry etching, the Cr-film mask was chemically removed and coplanar Au-electrodes were fabricated by electroplating. The geometry of electrode was set into the following values: width of hot electrode=5 μm , electrode gap=25 μm , interaction length=40mm, height of electrodes= about 20 μm .

In the wafer sample No. 1, three etching patterns and a reference pattern were fabricated on the wafer to investigate effective etching patterns for decreasing driving voltage. Schematic cross-sections and widths of patterned buffer layers are shown in Figure 3 and Table 1, respectively. Type R is the reference pattern for evaluating the effect of buffer layer patterning. Types A to C were the etching patterns having different etching widths. Type A was the pattern in which the

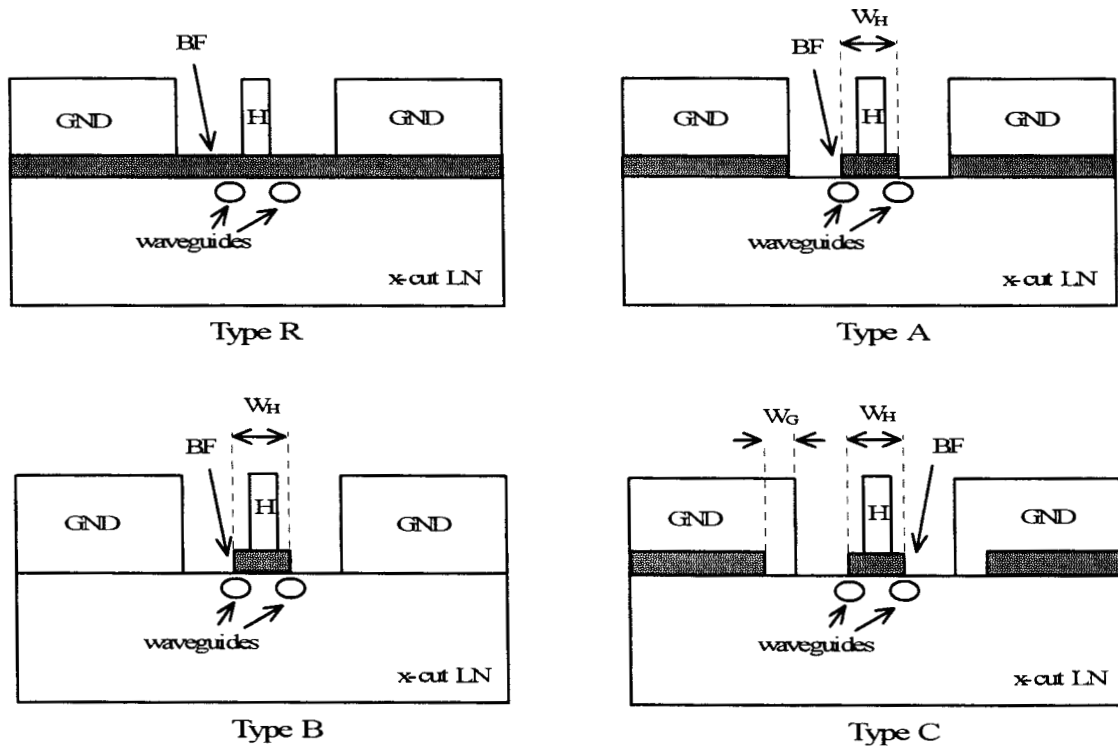


Figure 3 Schematic cross-sections of x-cut LN intensity modulator showing buffer layer structure of each configuration.

Table 1 Values W_H and W_G of each configuration fabricated on the wafer sample No. 1.

Configuration	W_H	W_G
Type R	---	---
Type A	13 μm	---
Type B	13 μm	---
Type C	7 μm	15 μm

Table 2 Measurement results of the wafer sample No. 1.

Configuration	Electrical Bandwidth (@ -3dB) [GHz]	n_m ---	Z_o [Ω]	V_π (@ 1kHz) [V]
Type R	4.90	2.36	54	4.8
Type A	4.96	2.36	56	4.8
Type B	4.61	2.41	55	4.1
Type C	4.61	2.41	56	4.7

buffer layer exposed between electrodes was removed, and most of buffer layer except for directly under and surrounding the hot electrode was removed in type B. Type C was an intermediate pattern of type A and B. These etching patterns were sequentially arranged on the wafer in order to expose them to the same wafer process.

After the wafer process, each of the modulator chips were diced from the wafer and mounted on cases. Electrical bandwidth effective refractive index of microwave (n_m), characteristic impedance of electrodes (Z_o) and halfwave voltage (V_π) were measured. A network-analyzer (HP8510C) was used for measurement of electrical bandwidth, and the n_m and Z_o were measured by time domain reflection of microwave. For measurement of V_π , polarization maintaining optical fiber (PMF) and single mode optical fiber (SMF) were attached to input and output end-surfaces of the chip, respectively. TE-polarized lightwave from 1.55 μm DFB laser diode was incident through the PMF and output from the SMF was incident on a photo-diode connected to an oscilloscope. The V_π driven at 1 kHz was measured from the sinusoidal response observed on the oscilloscope.

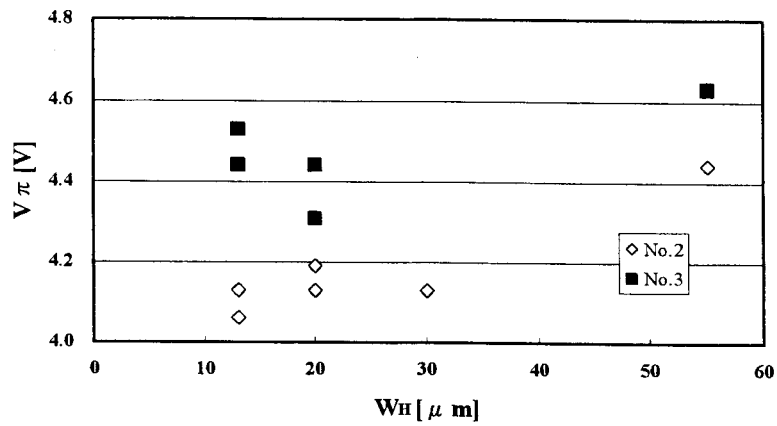
Measurement results on electrical bandwidth, n_m , Z_o and V_π of the wafer sample No. 1 are shown in Table 2. The V_π of type B was lowest and corresponded to about a 15% decrease to that of reference type R. A little degradation of the electrical bandwidth and n_m was observed in type B and C but it seemed to be not serious for 10G modulation. The Z_o was less affected by buffer layer patterning, From these results, type B was seen to be most effective in decreasing driving voltage without serious degradation of other characteristics,

In the wafer samples No.2 and 3, buffer layer width W_H of type B was selected as a parameter to decide optimum width for improving interaction between lightwave and microwave, Tested values of W_H are shown in Table 3. The wafer samples were fabricated in the same procedure of the wafer sample No.1. After dicing, the V_π and n_m were measured using probes.

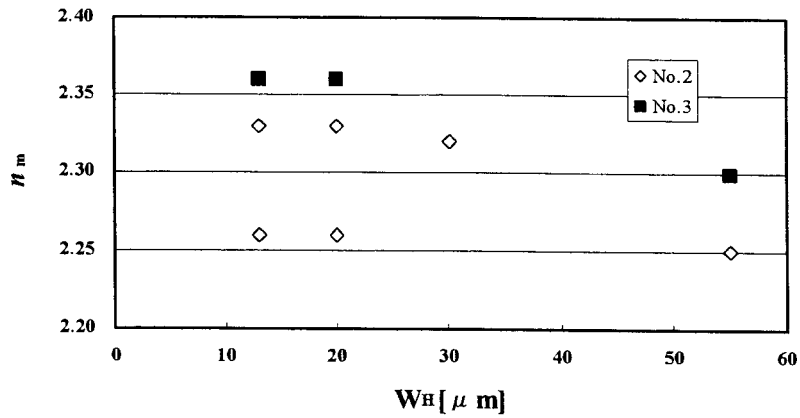
Table 3 Values W_H of each configuration fabricated on the wafer samples No.2 and 3.

Configuration	W_H
Type R	---
Type B13	$13\mu\text{m}$
Type B20	$20\mu\text{m}$
Type B30	$30\mu\text{m}$

Results of measurement are shown in Figures 4(a) and 4(b). As the value W_H got smaller, the V_{π} decreased gradually and the n_m somewhat degraded as shown in Figures 4(a) and 4(b). From this result and preliminary experiment described in the section of design concept, the V_{π} seemed to become lowest without serious degradation of bandwidth when the value W_H was set into around $13\mu\text{m}$.



(a)



(b)

Figure 4 Experimental results showing the relationships between the values W_H and characteristics of modulator chips.

(a) for V_{π} and (b) for n_m . Plots corresponding to $W_H = 55\mu\text{m}$ are the values of type R.

Table 4 Measurement results of fabricated modulators.

Sample No.	Configuration	Insertion Loss [dB]	On-Off E.R. [dB]	V_{π} (@ 1kHz) [V]	Optical Bandwidth (@ -3dB) [GHz]
R-1	Type R	4.6	30.2	4.9	11.1
R-2	Type R	4.5	29.6	4.6	9.2
R-3	Type R	4.0	33.4	4.6	9.5
B13-1	Type B13	4.3	31.7	4.2	7.3
B13-2	Type B13	5.4	30.5	4.4	7.3
B13-3	Type B13	4.8	34.6	4.4	7.8

3.3 Performance of Modulators

To evaluate the effect of patterned buffer layer configuration as the modulator, three chips of each type R and type B 13 (see Table 3) were selected from the wafer samples No.2 and 3 and fabricated into modulators. They were mounted on the case and a 50-ohm resistor and capacitor at the end point terminated their electrodes. PMF and SMF were attached to input and output end-surfaces of the chips, respectively, and fixed by ultra-violet cured adhesive. After hermetically sealing the package, characteristics of the fabricated modulators, such as insertion loss, on-off extinction ratio, V_{π} and optical bandwidth were measured. A 1.55/ μm DFB laser diode was used for measuring optical characteristics of modulators. The optical bandwidth was measured by a Hewlett-Packard optical component analyzer. After measuring their above-mentioned characteristics, dc-drift of the selected modulators was measured by auto-bias control method at 80°C for 100 hours.

Table 4 shows the measurement results of modulator characteristics. No difference on optical insertion loss and extinction ratio of each modulator was observed. Compared with type R, some degradation of optical bandwidth was observed in type B 13 but seemed to be not serious for 10G modulation. The V_{π} of types B13 was lower than that of type R corresponding to about 9 % decrease of driving voltage. These results confirmed that buffer layer patterning by dry etching

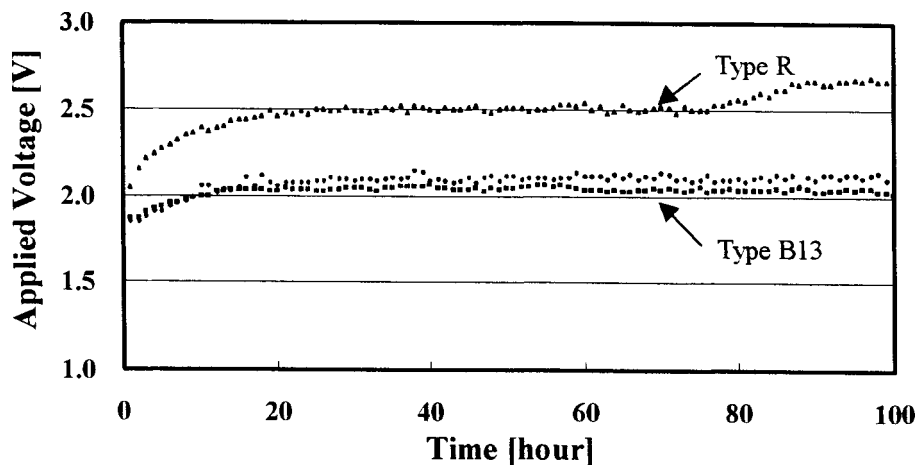


Figure 5 Results of dc-drift measurement of the modulators.

was effective in decreasing the driving voltage of the modulator without serious degradation of optical characteristics of them .

Figure 5 shows the results of dc-drift measurement of the modulators. It is obvious that applied dc bias voltage of type B13 was lower than that of type R. These results would confirm that the patterned buffer layer configuration was effective in dc-drift suppression as we expected.

4. CONCLUSION

According to above-mentioned experimental results, type B pattern in which most of the SiO₂ buffer layer except for directly under and surrounding the hot electrode was removed, might be the best configuration for decreasing driving voltage of the modulators. When the buffer layer width W_H was set to 13 μ m, a 9 to 15% decrease in driving voltage was achieved. Although the optical bandwidth of the modulators was somewhat degraded due to rising up of n_m , the degradation would be compensated by fabricating higher electrodes. It was also clarified that this configuration was superior to conventional modulators with planar buffer layer in their dc-drift characteristics. The reason for this advantage is uncertain but we consider that decreasing the total amount of electric carrier by buffer layer removal strongly assists the preventing leakage by buffer layer separation previously shown by Yamada and Minakata

ACKNOWLEDGMENT

Authors are thankful for staffs of LN production group of the optoelectronics division for their help on fabrication and measurement of LN modulators.

REFERENCES

1. S. Yamada and M. Minakata, "DC drift phenomena in LiNbO₃ optical waveguide devices," *Jpn. Jour App. Phys.* Vol. 20, pp. 733-737, 1981
2. H. Nagata, N. Mitsugi, J. Ichikawa, and J. Minowa, "Material reliability for high-speed lithium niobate modulators," *SPIE Proc. Optoelectr Integr. Circuits*. Vol. 3006, pp.301-313, 1997